Available online at www.sciencedirect.com
ScienceDirect
Polymer 48 (2007) 1844–1856
polymer
www.elsevier.com/locate/polymer

# Controlled polyethylene chain growth on magnesium catalyzed by lanthanidocene: A living transfer polymerization for the synthesis of higher dialkyl-magnesium

Thomas Chenal, Xavier Olonde, Jean-François Pelletier, Karel Bujadoux, André Mortreux*

*Unité de Catalyse et de Chimie du Solide, UMR CNRS 8181, ENSCL, Bâtiment C7, BP 90108-59652 Villeneuve d'Ascq Cedex, France*

Received 29 September 2006; received in revised form 25 January 2007; accepted 11 February 2007
Available online 14 February 2007

**Abstract**

The rare-earth metallocene chloride complexes $(C_5Me_5)_2LnCl_2Li(OEt_2)_2$ (Ln = Nd, Sm or Y) combined with an excess of dialkyl-magnesium compounds (butyl-ethyl-magnesium) afford active species for the polymerization of ethylene in alkanes or aromatic solvents at atmospheric pressure. A dynamic equilibrium between dormant species and a low concentration of catalytically active species is suggested to explain the living character of the polymerization process observed at temperatures up to 80 °C. A fluxional behavior of the polynuclear structure of the dormant species accounts for the fast and reversible exchange/transfer reaction of alkyl chains between lanthanide and magnesium metallic centers. The resulting mixture contains mainly di(polyethylenyl)magnesium compounds and can be directly used either for block copolymerisation with polar monomers or for any classical Grignard-like reaction for the synthesis of functionalized polyethylenes.


*Keywords:* Lanthanide; Transfer; Grignard

## 1. Introduction

Rare-earth complexes have been widely investigated as catalysts for polymerization [1] of various monomers including dienes [2], styrene [3] and polar monomers [4]. As regards the ethylene and α-olefins monomers, it is worth stating that group IV transition metal complexes have attracted much attention relative to their neighbours in the periodic classification [5]. The initial run up of the rare-earth metallocene polymerization catalysts started in late seventies and has met some success as it was considered as a good model for explaining the elementary steps in Ziegler–Natta polymerization (the ''lanthanide Ziegler–Natta model'') [6]. Fourteen electron species of the type $Cp_2LnR$ (dicyclopentadienyl-alkyl-lanthanide) are considered to mimic the isoelectronic $Cp_2ZrCH_3^+$ cationic species formed in the catalytic mixture of $Cp_2ZrCl_2$ and MAO (methylaluminoxane) [7]. Such species, for example $[Cp^*_2LuMe]_2$ [8] and $[Cp^*_2LaH]_2$ [9] (Cp*: pentamethylcyclopentadienyle), have proved to be very efficient for ethylene polymerization, despite their short lifetime. More stable aluminum adducts were also studied: the activity of the lutetium compound $Cp^*_2LuMe_2AlMe_2$ was attributed to a fast equilibrium with $Cp^*_2LuMe$, considered to be the real active species. However, the addition of only one more equivalent of $AlMe_3$ rendered the system totally inactive. In such lanthanidocene tetraalkyl-aluminate complexes, the alkyl exchange between terminal and bridging position has been well established [10]. This implies that all four alkyl groups may initiate successively the chain growth.

Chain growth on aluminum alone (the *Aufbaureaktion* described in Ziegler earlier work) [11] has been first shown to proceed on triethyl-aluminum, via a stepwise insertion of ethylene into the Al–C bonds at high temperature and pressure. A catalyzed version of this reaction has been proposed

* Corresponding author. Tel.: +33 (0) 320 43 49 93; fax: +33 (0) 320 43 65 85.
*E-mail address:* andre.mortreux@ensc-lille.fr (A. Mortreux).

0032-3861/$ - see front matter © 2007 Elsevier Ltd. All rights reserved.
doi:10.1016/j.polymer.2007.02.013

under less drastic conditions with transition metals [12], actinides [13], chromium [14] and recently with cationic yttrium complexes [15]. Similar chain growth reaction was also performed on dialkyl-zinc [16], alkyl-lithium [17] and dialkyl-magnesium [18]. The two latter compounds have the common point with the trialkyl-aluminum ones that they form aggregates [19]. In some cases, this aggregation ability was found to bother catalysis by the uncontrolled formation of inactive species, for example in ionic polymerization of styrene by lithium alkyl compounds [20] or in coordinative ring opening polymerization of cyclic esters by aluminum alkoxide compounds [21]. In contrast, aggregation of the catalytic species RLi with a metallic adduct of different nature, $MgR_2$, allowed the controlled polymerization of styrene by adjusting the ratio of the two components [22].

The work presented below can be considered as a further example combining several of the characteristics of the above catalytic combinations. First, the ethylene polymerization by lanthanide metallocene complexes will be shown to be controlled by adjusting the aggregation degree of the catalytic species with proper amounts of a dialkyl-magnesium additive. Second, as one of the first examples of catalyzed chain growth (CCG), a general concept recently developed by Gibson et al. [16b], this work will provide the possibility to synthesize oligomeric dialkyl-magnesium, which could be considered as an *Aufbaureaktion* on $MgR_2$ catalyzed by rare-earth metallocenes. Third, it will emphasize the initial idea proposed in our laboratory [23] and one other [24], consisting of the in situ formation of the active alkyl-lanthanidocene by alkylation of chlorolanthanidocene compounds, crystallized as their bis-[diethylether]lithium chloride adduct $Cp^*_2LnCl_2Li(OEt_2)_2$ **1** (Ln = Nd **1a**, Sm **1b** or Y **1c**) with butyl-ethyl-magnesium **2** (BEM). Unusual magnesium–lanthanide cooperation was revealed by running the ethylene polymerization process with a large Mg/Ln ratio and under mild conditions i.e. atmospheric pressure of ethylene, diluted solutions and temperature ranging from ambient temperature to 100 °C [25]. Detailed features of the lanthanidocene/BEM catalytic system for ethylene polymerization are presented here including (I) the living character of the polymerization, (II) the synthesis of di(polyethylenyl) magnesium($Mg(PE)_2$) and (III) some synthetic applications. Mechanistic implications are proposed based on the effect of several parameters on the catalytic system.

## 2. Experimental

### 2.1. Materials

All operations were performed under dry argon by using standard Schlenk techniques. Solvents were dried by passing through molecular sieves or by distillation from sodium benzophenone ketyl, under nitrogen, and were degassed by freeze-pump-thaw cycles prior to use. Ethylene (from Air Liquide) was purified by passing through molecular sieves and KOH. Carbon dioxide was purified by passing through molecular sieves. $SnCl_4$ was used as received from Aldrich. Methyl methacrylate (MMA) and ε-caprolactone (εCL) were purchased from Acros and were distilled over $CaH_2$ prior to use. Undec-1-ene (from Aldrich) was distilled over sodium prior to use. Lanthanidocene compounds $Cp^*_2LnCl_2Li(OEt_2)_2$ **1a–c** were synthesized according to a reported procedure [26]. BEM **2** was obtained from Texas Alkyl as 20 wt.% solution in heptane [27]. GPC was performed on a Waters CPG 150C apparatus equipped with Varian and Tosoh TSK columns. The eluent was 1,2,4-trichlorobenzene and the temperature was maintained at 135 °C. NMR spectra of polymer samples were recorded on a Bruker ASX400 spectrometer at 135 °C in 1,2,4-trichlorobenzene solutions, using either tetrachloroethane-$d_2$ or toluene-$d_8$ for internal lock. IR spectra were recorded as polyethylene films using a Perkin–Elmer 221 spectrometer. DSC was run on a Perkin–Elmer DSC7 instrument with a scanning rate of 10 °C/min. Mass spectra were recorded on a F.A.B. Kratos Concept II MM apparatus, in the negative mode, using triethanolamine matrix. GC analyses were performed with a Chrompack 9001 chromatograph equipped with a WCOT SIMDIST column and a flame ionization detector.

### 2.2. Ethylene polymerization

In a typical experiment (run 1), the anhydrous and degassed solvent (Isopar L, 500 mL) was placed in a thermostated (80 °C) glass vessel equipped with a powerful magnetic stirrer (1100 rpm). Ethylene inlet allowed to saturate continuously the inner medium at 10 cmHg above atmospheric pressure, i.e. 114 kPa. A catalytic mixture of $Cp^*_2NdCl_2Li(OEt_2)_2$ **1a** (64.1 mg, 0.1 mmol) and BEM **2** (2.76 g of the heptane solution, 5 mmol) was prepared under argon using usual Schlenk techniques and diluted in 10 mL of toluene at ambient temperature 1 h before being injected into the polymerization reactor. The ethylene consumption was then monitored with a flowmeter. The polymerization was stopped (96 min after the catalytic mixture injection) by hydrolysis with degassed water. The polymer was recovered by precipitation using 2 L of methanol acidified by 1 mL of concentrated HCl. The polymer was then filtered, washed with pure methanol, dried and weighed (44.1 g). GPC : $\overline{M}_n$ [PDI], 4400 g/mol [2.4]. NMR, IR: no branching detectable, vinyl terminations around 3% of the total chain ends or 0.1 double bond for 1000 C. DSC: mp = 134 °C, melting energy = 220 J $g^{-1}$. From a direct sampling after hydrolysis, no oligomers were found by gas phase chromatography. The same procedure was employed for runs 2–23 using conditions given in Tables 1–4. Only marked differences in the results of the polymer analyses for theses runs are reported in the corresponding tables.

### 2.3. Undec-1-ene homologation with ethylene

The ethylene polymerization was run with the samarium precursor $Cp^*_2SmCl_2Li(OEt_2)_2$ **1b** (0.1 mmol), BEM **2** (1.0 mmol), undec-1-ene (10 mmol) in toluene (100 mL) at 100 °C. Gas phase chromatography was performed on aliquots

taken with a syringe at different times and peaks were assigned by comparison of retention times with those of known alkanes and alkenes.

Table 1
Effect of the dialkyl-magnesium amount[a]

| Entry | Mg (mmol) | Time (min) | Weight (g) | $\overline{M}_n$ (g/mol) | $\overline{M}_w/\overline{M}_n$ |
|---|---|---|---|---|---|
| 2 | 0.2 | 5 | 9.6 | 2440 | 2.1 |
| 3[b] | 0.5 | 5 | 8.2 | 2820 | 1.6 |
| 4[b] | 1 | 5 | 4.4 | 1900 | 1.3 |
| 5[b] | 2 | 5 | 3.1 | 690 | 1.3 |
| 6[b] | 5 | 5 | 2.6 | 400 | 1.3 |
| 7[b] | 10 | 5 | 2.5 | nd | nd |
| 8a[c] | 5 | 1.67 | 1.1 | 485 | 1.2 |
| 8b[c] | | 8 | 5.5 | 580 | 1.2 |
| 8c[c] | | 18 | 10.2 | 900 | 1.2 |
| 8d[c] | | 20 | 11 | 950 | 1.3 |
| 8e[c] | | 22 | 13.5 | 1130 | 1.5 |
| 9a[c] | 1.1 | 1 | 0.7 | 540 | 1.3 |
| 9b[c] | | 2.5 | 2.2 | 970 | 1.3 |
| 9c[c] | | 5 | 3.6 | 1400 | 1.3 |
| 9d[c] | | 7 | 4.3 | 1640 | 1.4 |
| 10 | 1 | 2.5 | 2.3 | 990 | 1.3 |
| 11[d] | 1 | 5.5 | 2.3 | 980 | 1.3 |

[a] $(C_5Me_5)_2SmCl_2Li(OEt_2)_2$ **1b**: 0.1 mmol unless otherwise specified; butyl-ethyl-magnesium **2**; solvent: Isopar L 500 mL; ethylene: 113 kPa; temperature: 80 °C.
[b] The same run without quenching at 5 min is shown in Fig. 3.
[c] Twenty millilitres sampling of the same runs 8 and 9. The weight indicated is the ethylene amount measured by the flowmeter and was corrected to take into account the previous samples.
[d] $(C_5Me_5)_2SmCl_2Li(OEt_2)_2$ **1b**: 0.05 mmol.

Table 2
Number of growing polymer chains[a]

| Entry | Lanthanide (0.1 mmol) | BEM (mmol) | $m/\overline{M}_n$[b] (mmol) |
|---|---|---|---|
| 1e | Nd | 5 | 10.1 |
| 12 | Y | 5 | 12.5 |
| 13 | Sm | 5 | 11.9 |
| 5 | Sm | 2 | 4.5 |
| 9d | Sm | 1.1 | 2.6 |
| 4 | Sm | 1 | 2.3 |

[a] Conditions: see Fig. 1, Tables 1 and 3.
[b] $m/\overline{M}_n$ ratio between the consumed ethylene and the average molecular weight of the polymer samples before precipitation.

Table 3
Lanthanide and solvent variation[a]

| Entry | Ln | Solvent | Time (min) | Weight (g) | $\overline{M}_n$ (g/mol) | $\overline{M}_w/\overline{M}_n$ |
|---|---|---|---|---|---|---|
| 1e | Nd | Isopar L | 45 | 15.85 | 1560 | 1.3 |
| 12 | Y | Isopar L | 23 | 13.5 | 1080 | 1.5 |
| 13 | Sm | Isopar L | 35 | 13.5 | 1130 | 1.5 |
| 14 | Sm | Heptane | 65 | 12.6 | 1030 | 1.2 |
| 15 | Sm | Toluene | 120 | 34.7 | 2930 | 1.3 |
| 16 | Sm | Xylene | 90 | 27.2 | 3070 | 1.5 |
| 17 | Sm | Mesitylene | 80 | 37.6 | 3830 | 1.5 |

[a] $(C_5Me_5)_2LnCl_2Li(OEt_2)_2$ **1**: 0.1 mmol; butyl-ethyl-magnesium **2**: 5 mmol; solvent: 500 mL; ethylene: 113 kPa; temperature: 80 °C. Polymer properties were obtained for a 20 mL sampling at the starting precipitation, the weight indicated is the ethylene amount measured by the flowmeter at this time. The whole runs are depicted in Fig. 4.

Table 4
Temperature effect[a]

| Entry | Temperature (°C) | Time (min) | Weight (g) | $\overline{M}_n$ (g/mol) | $\overline{M}_w/\overline{M}_n$ |
|---|---|---|---|---|---|
| 18[b] | 0 | 48 | 1.6 | 2230[c] | 21[c] |
| 19a[d] | 40 | 8 | 1.3 | 740 | 1.2 |
| 19b[d] | | 30 | 5.8 | 1050 | 4.4 |
| 19c[d] | | 45 | 9.9 | 1560 | 22 |
| 20a[d] | 60 | 5 | 1.9 | 760 | 1.2 |
| 20b[d] | | 15 | 6.1 | 910 | 1.3 |
| 20c[d] | | 21 | 7.3 | 990 | 1.3 |
| 20d[d] | | 29 | 8.7 | 980 | 1.3 |
| 20e[d] | | 31.5 | 9.4 | 1050 | 1.4 |
| 20f[d] | | 34 | 10.8 | 1200 | 3.8 |
| 20g[d] | | 42 | 13.0 | 1400 | 8.1 |
| 21[e] | 100 | 3.7 h | 180 | 2110 | 2.0 |
| 22[e] | 112 | 3.5 h | 250 | 2000 | 2.0 |
| 23[e] | 140 | 4 h | 70 | 550 | 2.0 |

[a] $(C_5Me_5)_2SmCl_2Li(OEt_2)_2$ **1b**: 0.1 mmol; butyl-ethyl-magnesium **2**: 5 mmol otherwise specified; solvent: Isopar L 500 mL otherwise specified; ethylene: 113 kPa.
[b] Butyl-ethyl-magnesium **2**: 1 mmol; solvent: toluene 100 mL.
[c] The polymer did not fully dissolve in 1,2,4-trichlorobenzene at 135 °C and the reported molecular weight reflects only the soluble portion of the sample. Molar masses up to million g/mol were visible on the GPC curve.
[d] Twenty millilitres sampling of the same runs 19 and 20. The weight indicated is the ethylene amount measured by the flowmeter and was corrected to take into account the previous samples.
[e] Vinyl terminated polymer were detected by NMR: around 90 mol-% corresponding to unsaturation contents of 5.8, 6.4 and 23 double bonds for 1000 C for runs 21–23, respectively.

### 2.4. Polyethylenyl carboxylic acids ($H-(CH_2-CH_2)_n-COOH$)

Following the above-mentioned procedure using toluene as the solvent (500 mL), $Cp^*_2SmCl_2Li(OEt_2)_2$ **1b** as the lanthanide precursor (0.1 mmol) and 100 equivalents of BEM **2** (10 mmol), the ethylene polymerization was run at 80 °C during 7 min (90 mmol of ethylene were polymerized). Next, carbon dioxide was bubbled in the polymer solution for 2 h at the same temperature. Usual work-up gave 4.2 g of the functionalized polymer. IR: $\overline{\nu}_{C=O}$ 1710 $cm^{-1}$. $^1H$ NMR (400 MHz, 1,2,4-trichlorobenzene, tetrachloroethane-$d_2$): $\delta$ 12.64 ppm (R–COO*H*). $^{13}C$ {$^1H$} NMR (50 MHz, 1,2,4-trichlorobenzene, tetrachloroethane-$d_2$): $\delta$ 180 ppm (R–*C*OOH). Mass spectrometry: *m/z* [*n* in the parent ion formula $H-(CH_2-CH_2)_n-COO^-$] (abundance), 129 [3] (18), 157 [4] (60), 185 [5] (98), 213 [6] (100), 241 [7] (86), 269 [8] (58), 297 [9] (38), 325 [10] (22), 353 [11] (13), 381 [12] (8), 409 [13] (5); *m/z* [*n* in the fragmentation ion formula $H-(CH_2-CH_2)_n^-$] (abundance), 169 [6] (8), 197 [7] (19), 225 [8] (30), 253 [9] (41), 281 [10] (45), 309 [11] (44), 337 [12] (37), 365 [13] (28), 393 [14] (20), 421 [15] (14), 449 [16] (9), 477 [17] (6).

### 2.5. Star-shaped polymer ($((H-(CH_2-CH_2)_n)_4Sn$)

The ethylene polymerization was run with the samarium precursor $Cp^*_2SmCl_2Li(OEt_2)_2$ **1b** (0.1 mmol), BEM **2** (5.0 mmol) in Isopar L (500 mL) at 80 °C during 25 min

(400 mmol of ethylene were polymerized). A control sample was taken with a syringe. Then, $SnCl_4$ (2.5 mmol) was slowly dripped in the mixture over several minutes. After 1 h reaction at 80 °C, a usual work-up afforded 11.4 g of star-shaped polymer. GPC : $\overline{M}_n$ [PDI], 940 g/mol [1.2] (control sample), 2560 g/mol [1.5] (star-shaped polymer). The following analysis was performed on the product obtained under similar conditions, but with only 60 mmol of ethylene. $^{13}C$ {$^1H$} NMR (50 MHz, toluene-$d_8$): $\delta$ 9.6 ppm ((R−$CH_2$−)$_4$Sn), 14.4 ppm ($CH_3$−), 16.6 ppm ((R−$CH_2$−)$_3$Sn−), 23.2 ppm ($CH_3$−$CH_2$−), 27.6 ppm ((R−$CH_2$−$CH_2$−$CH_2$−)$_4$Sn), from 29.9 to 30.2 ppm ((−$CH_2$−)$_n$), 32.4 ppm ($CH_3$−$CH_2$−$CH_2$−), 35.1 ppm ((R−$CH_2$−$CH_2$−)$_4$Sn).

### 2.6. Ethylene and methyl methacrylate diblock copolymer (PE−PMMA)

The ethylene polymerization was run with the samarium precursor $Cp^*_2SmCl_2Li(OEt_2)_2$ **1b** (0.1 mmol), BEM **2** (5.0 mmol) in Isopar L (500 mL) at 80 °C during 30 min (440 mmol of ethylene were polymerized). A control sample was taken with a syringe before the temperature was decreased to −78 °C. Then methyl methacrylate (50 mmol) was carefully added and allowed to react at the same temperature for 2 h. The usual work-up gave 16.7 g of material. GPC : $\overline{M}_n$ [PDI], 1040 g/mol [1.2] (control sample), 1450 g/mol [1.4] (material). The crude copolymer was then submitted to an extraction using refluxing acetone during 4 days in a Kumagawa apparatus. A 47% weight loss was observed and the insoluble fraction had a polydispersity index of 1.1. IR analyses confirmed the presence of both types of polymer in the insoluble product.

### 2.7. Ethylene and ε-caprolactone diblock copolymer (PE−PεCL)

The ethylene polymerization was run with the samarium precursor **1b** $Cp^*_2SmCl_2Li(OEt_2)_2$ (0.1 mmol), BEM **2** (5.0 mmol) in Isopar L (500 mL) at 80 °C during 30 min (430 mmol of ethylene were polymerized). A control sample was taken with a syringe before the addition of ε-caprolactone (500 mmol). After 1 h reaction at 80 °C, the usual work-up afforded 60 g of material. GPC : $\overline{M}_n$ [PDI], 1100 g/mol [1.2] (control sample), 4280 g/mol [12.7] (material). The crude copolymer was then submitted to an extraction using refluxing acetone during 8 days in a Kumagawa apparatus resulting in an 88% loss of weight. The extract remained bimodal (PDI = 12.4) while the insoluble fraction had a polydispersity index of 1.3 and $\overline{M}_n$ = 1760. DSC and IR analyses confirmed the presence of both type of polymer in the insoluble product.

## 3. Results

### 3.1. Living character study

All polymerization experiments started under stirring by the injection of the catalytic mixture consisting of the lanthanidocene chloride **1** and the alkylating agent **2** in a glass vessel containing the solvent saturated with ethylene under stirring at atmospheric pressure. A flowmeter on the ethylene feed allows to follow the ethylene consumption. An example of the ethylene consumption curve is depicted in Fig. 1 for run 1.

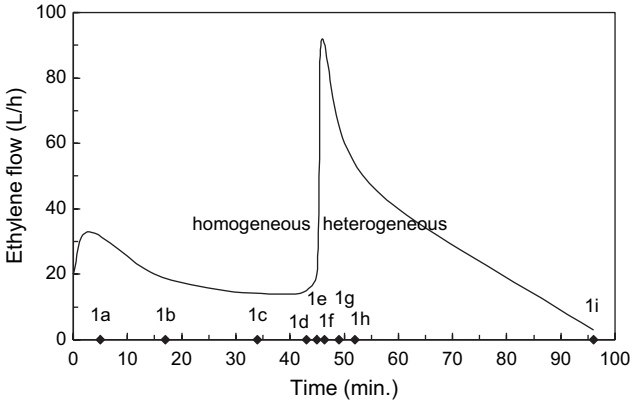


Fig. 1. Ethylene consumption during run 1. Conditions: $(C_5Me_5)_2NdCl_2$-$Li(OEt_2)_2$ **1a**: 0.1 mmol; butyl-ethyl-magnesium **2**: 5 mmol; solvent: Isopar L 500 mL; ethylene: 113 kPa; temperature: 80 °C. Intermediate points 1a–1h were obtained from a 20 mL sampling of the run, followed by a scaled work-up.

One can easily distinguish two parts, which can be related to the physical state of the polymerization medium. During the first part, the medium is homogeneous, transparent and colored according to the lanthanide used: light blue for Nd, orange for Sm, colorless for Y. The second part is characterized by a heterogeneous medium (white precipitate). After an equilibration period at the early stage of the run, the rate of ethylene consumption remains constant during a time which will be shown dependent on the magnesium content, before a sharp increase occurring at the beginning of precipitation. In cases where precipitation could be avoided (vide infra, at higher temperature), a steady state ethylene consumption was observed for several hours.

Sampling the polymerization medium of run 1 (entries 1a–1i in Table 1) gave more details about the polymerization process. Analyses of the samples by size exclusion chromatography allowed to trace the graph representing the average length of polymer chains ($\overline{M}_n$) versus the polymer weight (measured by integration of ethylene consumption) (Fig. 2, left part).

Apart from the first point, the curve is a straight line. The deviation of the first point might be attributed to the presence of light oligomers which cannot be detected. Even if the average molecular weight grew regularly, the mass distribution was not always uniform during the process as exemplified in Fig. 2, right part. In the homogeneous stage (samples **1a–d**; thin lines) unimodal and narrow distributions were found, proving that, statistically, all chains grew steadily. However, the values circa 1.2 for the polydispersity index (PDI = $\overline{M}_w/\overline{M}_n$) were noticeably higher than expected for perfect statistics corresponding to a Poisson distribution (1.0). Then, when the medium became heterogeneous (samples **1f–h**, thick lines), the distribution turned to be bimodal: a second hump appeared, showing that some chains are growing more rapidly than the others. However, it is also noteworthy that the low

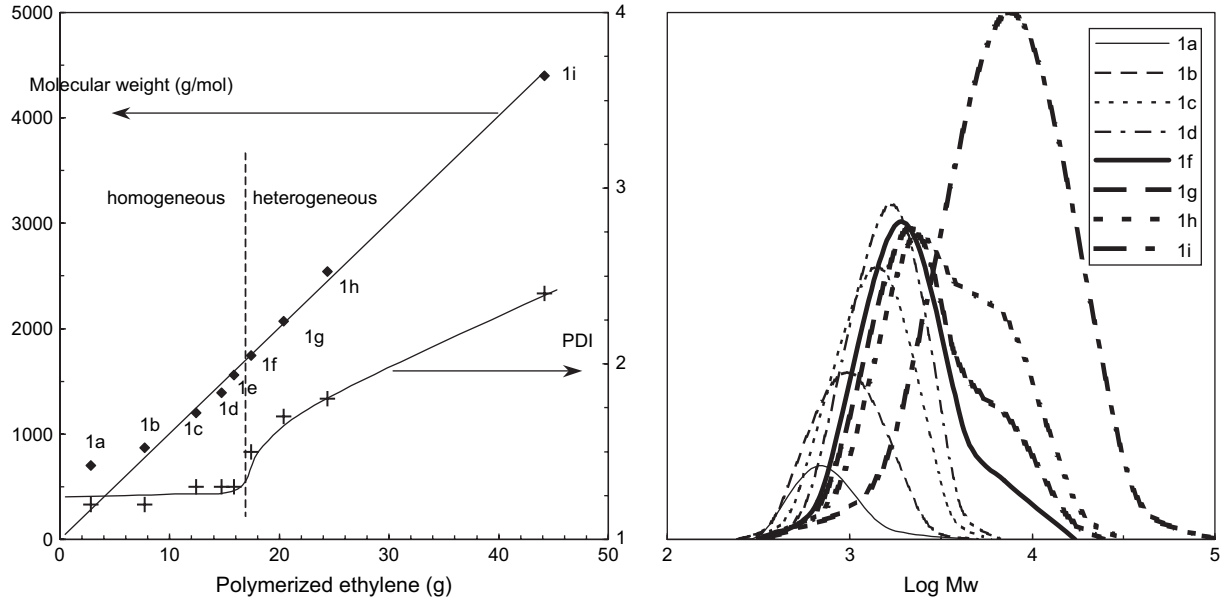


Fig. 2. Living character study. Molecular weight, polydispersity index and mass distribution by GPC analysis of the samples from run 1 (conditions: see Fig. 1).

masses hump disappeared progressively. At the end of the process (final polymer **1i**), the distribution was again unimodal, with a polydispersity index of 2.4. These GPC data indicate that each polymer chain was growing all along the process but grew only at a slow rate in the homogeneous stage, up to molar masses of around 1400 g/mol. This rate became faster in the heterogeneous stage, giving higher polymer chains. The major part of the applications presented below will deal with results obtained in the homogeneous stage, after the initial equilibration period.

### 3.2. Effect of BEM concentration

Earlier studies already pointed out that the dialkyl-magnesium amount had much effect on the characteristics and the amount of the polymer obtained [23]. In this work, a more detailed and systematic study of this effect has been performed (runs 2–7 in Table 1).

The analysis of the ethylene consumption curves in Fig. 3, left part, shows a decrease of the activity with a concomitant lengthening in time of the homogeneous stage obtained for experiments involving higher amounts of BEM.

This series of curves indicates that an excess of BEM reduces the ethylene consumption rate. In the second step, after the precipitation has occurred, the ethylene consumption reaches a maximum, which is more or less at the same level.

### 3.3. Number of growing polymer chains

As far as the polymers obtained with different BEM amounts are concerned, the study of the average molecular weight versus the polymer production is very informative. In Fig. 3, right part, is plotted the average molecular weight of the polymer versus the amount of polymer during reactions involving the use of 1 mmol and 5 mmol Mg, corresponding to runs 8 and 9 in Table 1. The two straight lines indicate first that in both cases, a living process is occurring and second that, from the ratio between the two slopes (circa 5), the molecular weight is closely related to the amount of magnesium. Table 2 compares the number of the growing polymer chains

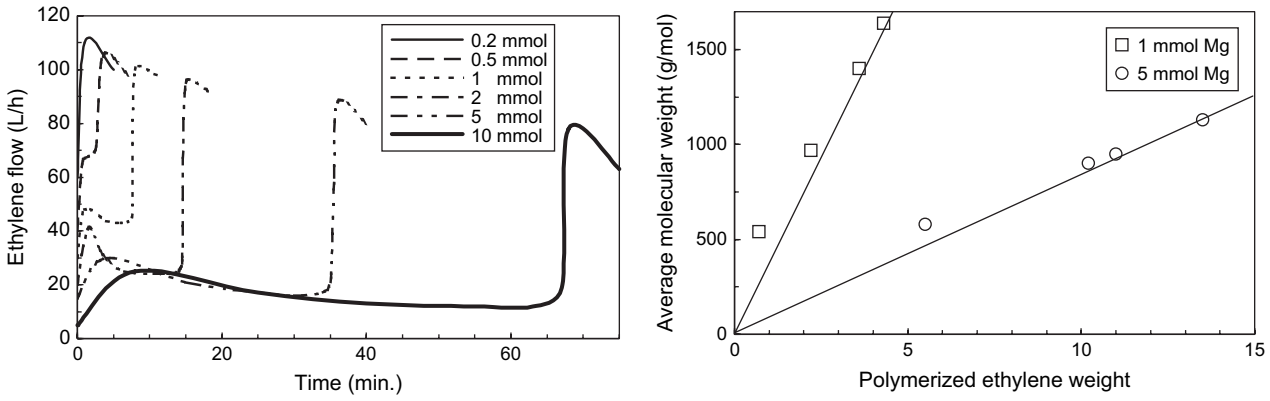


Fig. 3. Effect of the dialkyl-magnesium amount. Ethylene consumption and living character study. Conditions: see runs 2–7 in Table 1 without quenching at 5 min.

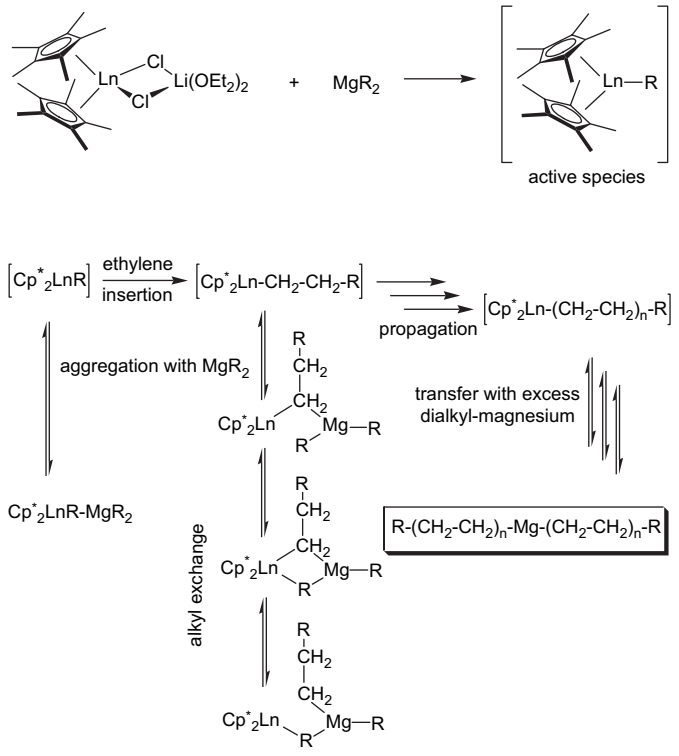


Scheme 1. Proposed reaction mechanism.

(the slopes of the above-mentioned straight lines) upon using different lanthanide precursors and different BEM concentrations.

One can notice that the calculated growing chain number is almost the same as the number of the alkyl groups which can be delivered by the Grignard reagent. Thus, all of the alkyls supplied by BEM, whatever their amount, are each used as initiator for the polymerization.

The linear relationship between chain lengths and polymer weights suggests first a living chain growth; the narrow molecular weight distribution observed in the first stage where a steady state ethylene consumption is also observed, as well as values of the alkyl chain number identical to that of the alkyl groups available from the magnesium dialkyls is consistent with a reversible transfer reaction between the magnesium dialkyl/polyethylenyl compound and the mononuclear lanthanidocene alkyl/polyethylenyl propagating species. This exchange must be rapid as compared with the propagation rate, and is probably occurring via polynuclear alkyl bridged intermediates. Since the reaction rate decreases with an increase of the Mg/Ln ratio, these polynuclear Ln–Mg bridged complexes must be considered as dormant species. Their structure is based on the usual ones of magnesium or aluminum alkyls, including bimetallic structures [19]. The proposed reaction mechanism is depicted in Scheme 1.

Whatever the structure of these intermediates be, well-controlled polymerization processes are obtained with systems in which active species are in very low concentration but in equilibrium with dormant species with a fast exchange rate. Linkage of the polymer chain to both lanthanide and magnesium will allow for the synthesis of functionalized polymer and block copolymers (see Section 3.9). Unlike ATRP [28] and group transfer polymerization [29], which imply radical and anionic mechanisms, respectively, the present controlled process is based on a coordination/insertion mechanism.

### 3.4. Lanthanide and solvent variation

$Cp^*_2LnCl_2Li(OEt_2)_2$ catalytic precursors **1b** (Ln = samarium, run 13) and **1c** (Ln = yttrium, run 12 in Table 4) were compared with **1a** (Ln = neodymium) under the same conditions.

The corresponding ethylene consumption curves are depicted in Fig. 4, left part. The same shape was observed: a homogeneous stage with a steady state ethylene consumption followed by a strong enhancement when the precipitation started. These rates at the end of the first stages were in the order Y > Sm > Nd. However, the polymer characteristics were similar.

Various solvents were also tested (see Fig. 4, right part, and runs 13–17 in Table 3). It appears from the GPC data that dialkyl-magnesium compounds $Mg(PE)_2$ just before precipitation had longer alkyl fragments in aromatic solvents ($\overline{M}_n$ > 3000 g/mol, runs 15–17) than in aliphatic ones ($\overline{M}_n$ ~ 1100 g/mol, runs 13 and 14). Within each class of solvent, the higher their boiling point, the longer alkyl fragments and the higher ethylene consumption rate were observed.

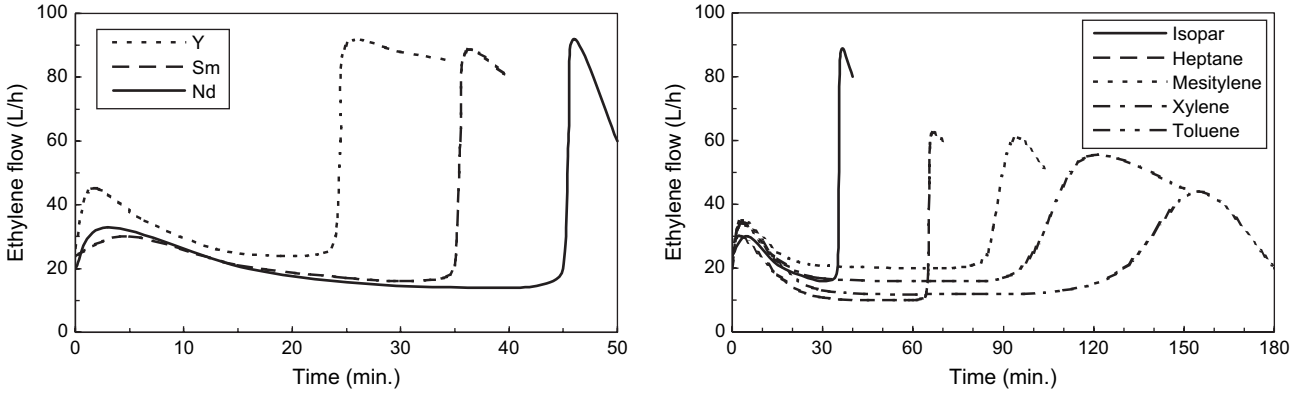


Fig. 4. Ethylene consumption: comparison between several lanthanidocenes and between several solvents. Conditions: see runs 1 and 12–17 in Table 3.

### 3.5. Temperature effect

The temperature effect on the polymerization rate is shown in Fig. 5, left part, by ethylene consumption curves versus time for the samarium precursor **1b** and in the right part of Fig. 5 which presents the evolution of the activity according to the temperature for different dialkyl-magnesium amounts associated with the neodymium precursor **1a** (neodymium).

In the high temperature range (above 100 °C) the precipitation was avoided owing to the better solubility of the polymers and to the relatively low molecular weights due to the occurrence of a transfer to monomer process (vide infra). One could notice the stability of the catalytic system during several hours without any decrease of activity. For run 22, the reaction had to be stopped because of the viscosity enhancement of the homogeneous solution (*250 g PE in 500 mL of solvent*). The optimum of activity near 110–120 °C can best be seen in Fig. 5, right part. The results presented in this figure were obtained with a set of complementary experiments where the temperature was varied all along the polymerization process. The data correspond to values related to steady state ethylene consumption at the corresponding temperature and Mg/Nd ratio. The right part of the curve obtained with the lowest magnesium amount (over 115 °C) denotes that irreversible deactivation is occurring, since the ethylene consumption could not be stabilized and slowly decreased with time. Hence, the presence of dialkyl-magnesium compounds in excess appears to be necessary to prevent irreversible deactivation at high temperature.

Considering the experiments conducted in the low temperature range (runs 18–20), three different observations lead to the same interpretation. First of all, in contrast with reactions conducted at 80 °C where the precipitate appears suddenly, at 60 °C the precipitate is gradually formed over several minutes. For temperatures below 40 °C, precipitation already starts slightly at the beginning of the experiments. Second, the chain number calculated from polymer yield and average molecular weight (see Fig. 6, left part) is close to the number of alkyl–metal bonds present in solution at 80 °C, while at 60 °C and worse at 40 °C, this chain number is much lower than the number of alkyl-magnesium units. This means that some alkyl-magnesium groups had not the opportunity to grow rapidly enough to give polymer chains. Finally, the mass distributions for the experiment carried out at 40 °C (see Fig. 6, right part) have a bimodal shape: a first distribution appears near

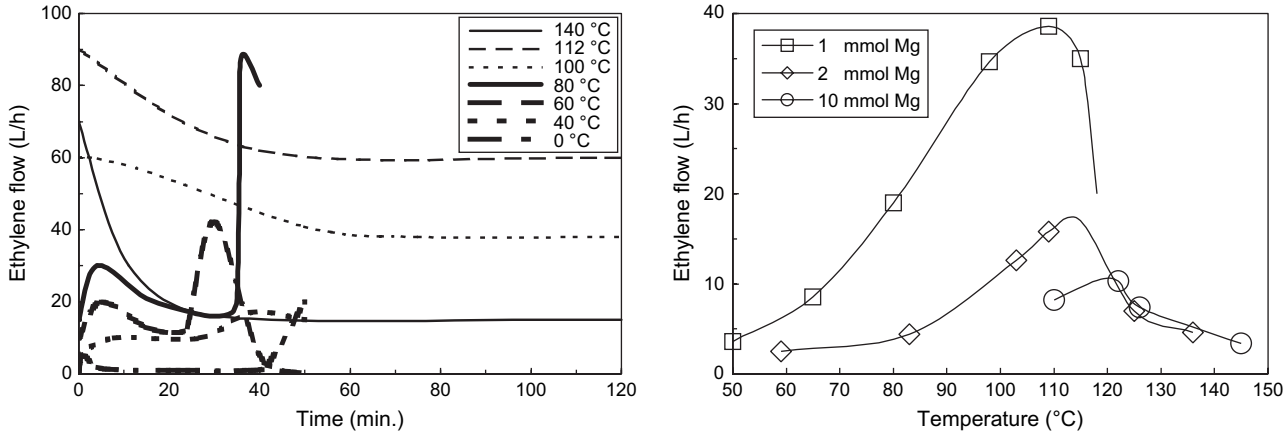


Fig. 5. Temperature effect. Left: ethylene consumption for identical BEM amounts. Conditions: see run 13 in Table 3 and runs 18–23 in Table 4. Right: steady state ethylene flow for different magnesium concentrations. Data points indicate the temperatures for which equilibration was waited to have a steady state ethylene consumption. Conditions: 50 μmol of the neodymium precursor **1a** in 25 mL of isododecane under 114 kPa of ethylene.

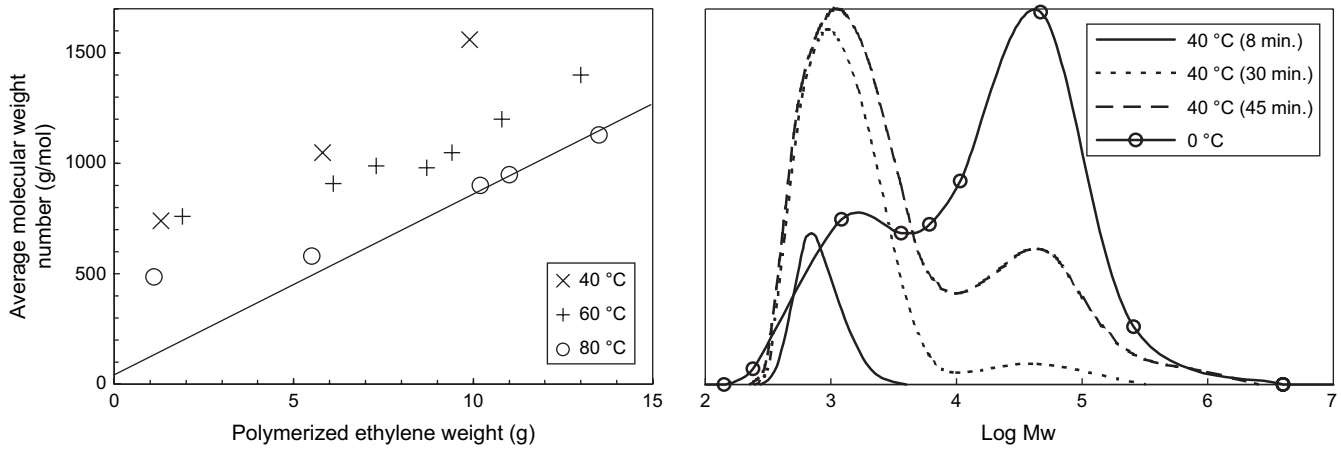


Fig. 6. Temperature effect: molecular weight and mass distribution of samples from runs 18–20, Table 4 and run 8, Table 1.

1000 g/mol (PDI = 1.2) at the beginning of the experiment; then a second distribution near 50,000 g/mol, becoming more and more important with time, enlarges the polydispersity indexes. This heavy polymer chain corresponds to the gradual formation of the precipitate. Compared with the mass distribution profiles obtained at 80 °C where the bimodal distributions have values corresponding to circa 1400 and 4400 g/mol (see Fig. 2, samples **1f–h**), the molar mass difference between the light and the heavy distributions is much more pronounced at 40 °C. All these observations (precipitation time, variation of the growing chain number, and monomodal vs. bimodal mass distribution) are consistent with the fact that two different regimes appear successively at 80 °C, whereas both are occurring simultaneously at lower temperature.

The experiment run at 0 °C (entry 18, Table 4), gives the limits of the lanthanidocene/dialkyl-magnesium catalytic system in the lower temperature domain. The first stage (see Fig. 5), which is lasting 40 min with an ethylene consumption almost negligible, looks like an induction period. As a result, the final polymer was found to be partly insoluble in 1,2,4-trichlorobenzene at 135 °C and the soluble part showed, by GPC analysis (see Fig. 6), some very high molar mass polyethylene, higher than $10^6$ g/mol. Similar results have already been obtained previously for ethylene polymerization catalyzed by lanthanides [30]. The GPC curve reflects a broad distribution (PDI = 21) corresponding to an uncontrolled process.

As far as the control of the chain growth transfer polymerization is concerned, the above results related to the temperature effect are of interest for a better understanding of the reversible chain growth process, as well as for others related to the occurrence of a exchange reaction between a polymerization catalyst and main group metal moieties used in excess for a living transfer polymerisation. Namely, a good control of the living character of a chain transfer polymerization is only obtained when the transfer reaction rate is much higher than the propagation rate. The relations between the transfer efficiency and the polydispersity were described for example in the case of ring opening polymerization of cyclic esters [31]. In our case, the polydispersity index observed during the first stage of a typical polymerization run (80 °C, PDI = 1.2 in run 1), evidences that the transfer rates are in agreement with the above criteria.

The experiments conducted at lower temperatures (runs 18–20 at, respectively, 0 °C, 40 °C and 60 °C) gave valuable insight on the evolution of the kinetic ratio between the ethylene insertion and the alkyl exchange reaction rates. Qualitatively, when the reaction temperature is lowered from 80 to 40 °C, the observation of earlier and gradual precipitation, the lower number of growing chains (Fig. 6) and the broader mass distribution suggests that the exchange rate decreases more rapidly than the insertion rate from 80 °C to 40 °C. As a result, the high overall polydispersity index (i.e. PDI = 21 at 0 °C) can be attributed to a low transfer rate, and consistent with the well known high intrinsic activity [9] of the active centers even at low temperature. In terms of activation energy, the insertion/propagation reaction must have a lower barrier than the exchange reaction. These results also mean that if one would be interested in such transfer reactions, doing experiments at different temperatures may have a strong influence on the overall process upon tuning the relative propagation to transfer reaction rates and therefore allow or not a reversible and controlled chain growth transfer.

### *3.6. Requirements for an efficient and controlled living transfer reaction*

Some conditions must be fulfilled to have a controlled molecular weight using the $Cp^*_2LnCl_2Li(OEt_2)_2$/BEM combination. They can be deduced from the analysis of the reaction mechanism depicted in the previous scheme. The curve (ethylene consumption) vs. time for all reactions conducted at 80 °C (Fig. 1) is fully consistent with a sudden, sharp increase in the amount of active propagating species. A rather stable ethylene consumption is observed at the beginning of the reaction, where all the process is occurring in an homogeneous phase, that is when the equilibria depicted in Scheme 1 are occurring. Deviation from this ideal situation is occurring suddenly when the catalytic solution becomes cloudy, due to precipitation of part of $Mg(PE)_2$ compound, via an equilibrium displacement. Due to this precipitation, the concentration of dialkyl-magnesium in solution decreases, resulting in an increase in mononuclear active $Cp^*_2Ln$-R species, which rapidly insert ethylene to produce higher molecular weight polymer. This results in a bimodal distribution (see Figs. 2 and 3), which finally lasts with a broad, but unimodal one at the end of the ethylene consumption. The occurrence of a stable polymerization process is viable only if the amount of dialkyl-magnesium is large enough to provide a control of the amount of active species: similar phenomena are occurring at different reaction times, according to the Mg/Nd ratio (Fig. 3), but also depend on the nature of the lanthanide catalyst, as well as that of the solvent (Fig. 5). These differences are most probably due to the aggregation ability of the Ln-R/$MgR_2$ systems, which depends on the metal and the solvent, which has, in addition, different solubilizing properties towards the polyethylenyl Grignard compounds produced during the process.

Therefore, the aggregation ability of the system is a key factor for controlling the activity and stability of the polymerization process. Two ways can be used to dissociate aggregates: dilution and addition of coordinating solvent. The first one is exemplified by simply adding solvent during one run which results in an increase of the reaction rate (see Fig. 7). This diluting effect corresponds to a higher dissociation degree of the Ln–Mg aggregative structures. The second one concerns the use of a coordinating solvent such as THF, which may exert a strong influence on the mononuclear dialkyl-magnesium and/or alkyl-magnesium–alkyl-lanthanide aggregates. When used in excess (THF/Ln = 10), such a O-donor ligand is known to reduce the activity of well-defined alkyl-lanthanidocene species via coordination on the metallic center, but not completely inhibiting polymerization [8a]. In our hands (see Fig. 7), using two equivalents of THF per magnesium, that is a *forty* fold excess vs. Nd, resulted in a marked and short living enhancement of the ethylene consumption. This

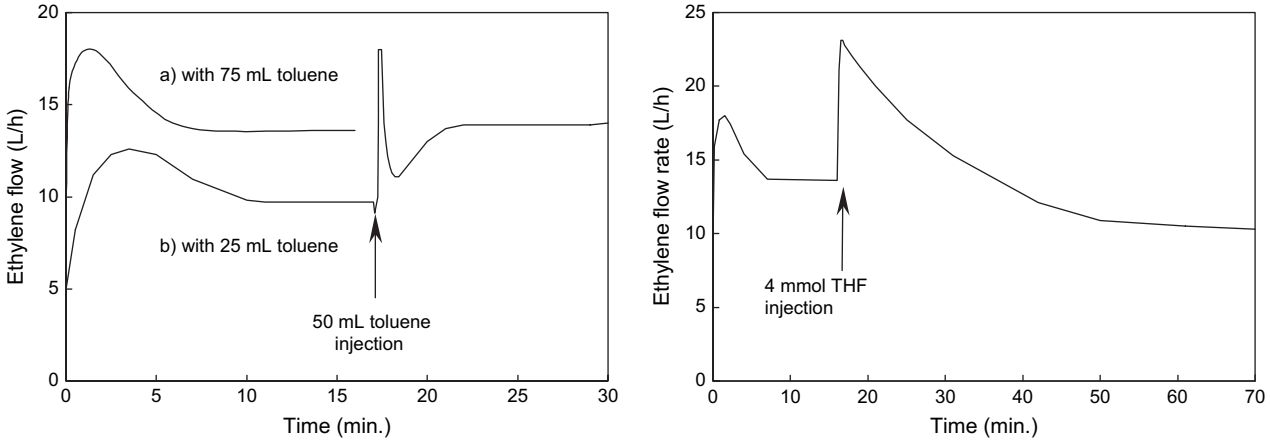


Fig. 7. Effect of dilution and addition of coordinating solvent on the ethylene consumption. Conditions: $(C_5Me_5)_2NdCl_2Li(OEt_2)_2$ **1a**: 0.1 mmol; butyl-ethyl-magnesium **2**: 2 mmol; ethylene: 114 kPa; temperature: 100 °C. The medium was always homogeneous.

promoter effect of THF can be rationalized by the coordination of the ether ligands to the dialkyl-magnesium compounds allowing the displacement of the equilibrium from the dormant heterometallic aggregates to a Mg–THF adduct along with free Ln-alkyl moieties, resulting in the activity enhancement.

### 3.7. Polymer properties

The hydrolysis and work-up of the usual polymerization medium (for example run 1 in Table 1) afforded polyethylene with the following features: sharp melting points around 134 °C, high density (>0.96) and high crystallinity (melting energies of 220 J $g^{-1}$). The IR and NMR data did not provide evidence for any branching. The double bond amount for this polymer obtained at 80 °C was found to be very low: 3% of chain ends were vinyl terminated at the end of run 1, which corresponds, for this polymer with $\overline{M}_n = 4400$ g/mol, to an unsaturation content of 0.1 double bond for 1000 carbon atoms. Similar results, though with some deviations, were found for the other runs up to run 20. However, α-olefins, i.e. vinyl terminations, are found at higher temperatures: around 6 double bonds for 1000 C at 100 and 112 °C (runs 21 and 22) and up to 23 double bonds for 1000 C at 140 °C (run 23). This corresponds, taking into account the $\overline{M}_n$ for those three runs, to ca 90% vinyl terminations. The classical process, which accounts for vinyl end group formation, is generally ascribed to β-hydrogen elimination. The generated hydrido-lanthanide species act as a new initiator for a new polymer growing chain, so that the whole reaction is a transfer to monomer process. The transfer reaction to ethylene can also be estimated by the increase of polymeric chain number: $m/\overline{M}_n = 8.5$, 125 and 127 mmol, respectively, at the end of runs 21 (100 °C), 22 (112 °C) and 23 (140 °C), while at 80 °C, the polymeric chain numbers using any of the three precursors **1a–c** are only slightly higher than the number of alkyl-metal initiating species (10 mmol): $m/\overline{M}_n = 10.1$ (neodymium, run 1e), 11.9 (samarium, run 13) and 12.5 mmol (yttrium, run 12 in Table 2). In the absence of dialkyl-magnesium in excess, using well-defined alkyl-lanthanidocene, the transfer reaction to ethylene usually occurs at lower temperatures [32].

Another striking point in this work is that experiments were not altered by catalyst deactivation through π-allyl complex formation in the presence of vinylic compounds [33]. Taking into account the double bond level and the weight of polymer at the end of each run, the olefin concentrations were estimated to be 0.15 mol $L^{-1}$ for run 21 and 0.23 mol $L^{-1}$ for runs 22 and 23. In fact, traces of internal double bonds could be detected by NMR (5% max. of the double bond content in runs 21–23). This means that, due to peculiar experimental conditions, the possible π-allyl complexes can insert ethylene by shifting the $\eta^3$-coordination mode to a $\eta^1$ mode of binding, as it has been already reported in other cases [34].

### 3.8. Ethylene polymerization in the presence of α-olefins

Following earlier reports on α-olefins polymerization with well-defined lanthanidocenes [10a], we checked that propylene could not be polymerized with the lanthanidocene **1** and dialkyl-magnesium **2** mixture [35]. In addition, attempts to copolymerize ethylene and but-1-ene failed [23], since the polymers obtained were always highly linear polyethylene. However, in these experiments conducted at high pressure and high temperature (1200 bar, 200 °C), a transfer mechanism to butene was evidenced by the lowering of the average molar mass obtained when the butene content of the feed was increased. This transfer to monomer process may be a useful way to incorporate α-olefins in the polymer chain, as it has been reported in zirconocene chemistry [36].

Fig. 8 gives the chromatogram of the oligomeric fraction of the polymer obtained during run 24 (Table 5) where undecene has been introduced at the beginning of the reaction.

Evidence is given for an oligomer distribution with an odd number of carbon atoms, along with the usual even distribution arising from the lanthanidocene/BEM catalyst. Undec-1-ene incorporation is obviously occurring to account for the odd number chain distribution. Since methyl branches were not detected in the polymer, only 1,2-insertion seems to be

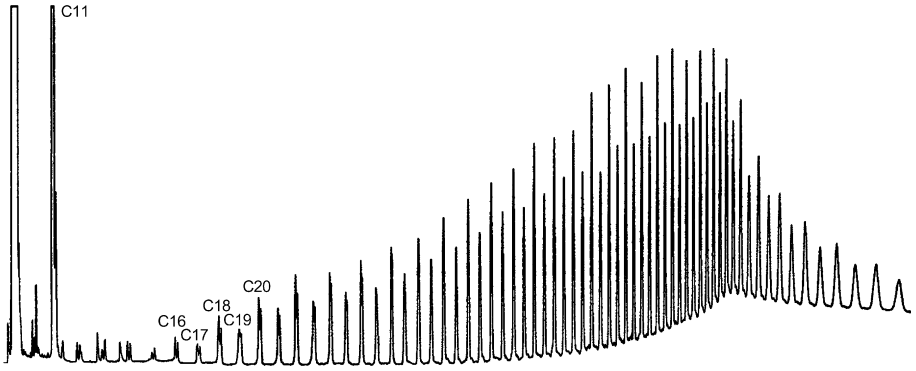


Fig. 8. Gas chromatography plot of the oligomeric fraction of the polymer obtained for the homologation of undecene (run 24 in Table 5).

effective. We can therefore conclude that, in our experimental conditions, α-olefins can insert into lanthanide hydride bonds but *not* into lanthanide carbon bonds, while ethylene can be inserted in both types of bonds. Such trends have been clearly elucidated earlier from NMR and field desorption mass spectrometry analysis of poly(ethylene-$d_4$) obtained in the presence of pent-1-ene with a samarocene catalyst [37].

### 3.9. Applications of $Mg(PE)_2$ compounds

Considering an ethylene polymerization conducted at 80 °C using BEM in excess, during the first stage, the net result before hydrolysis consists of polyethylenyl fragments bonded to lanthanide and most of them to magnesium. The behavior of these magnesium compounds was studied by testing typical reactions, reported in Table 5.

The polymerization reaction mixture behaves in a very similar manner as Grignard's compounds during addition of carbon dioxide and halide substitution in $SnCl_4$. The expected products are obtained in good yields and with satisfactory analytical properties. Carboxylic acids obtained in run 25 (Table 5), were analyzed by IR, NMR (see Section 2.4) and by mass spectrometry (Fig. 9).

The major distribution in the mass spectrum is attributed to the parent ions of formula $H-(CH_2-CH_2)_n-COO^{\bullet -}$. The ethylene unit number, $n$, was detected between 3 and 13. The maximum abundance was observed for $n = 6$, in accordance with the expected average molar mass (BEM: 10 mmol, functionalized polymer: 4.2 g, expected average molar mass: 210 g/mol, $H-(CH_2-CH_2)_6-COO^{\bullet -}$: 213 g/mol). Another distribution is superimposed with lower abundance and higher masses than the first one. It is attributed to fragmentation ions of formula $H-(CH_2-CH_2)_n^{\bullet -}$ and most probably corresponds to the result of a $CO_2$ loss from the parent ions. In this distribution, $n$ was detected between 6 and 17, with a maximum abundance of 45 for $n = 10$.

A star-shaped polyethylene was obtained via a transmetallation using $SnCl_4$ (run 26, Table 5) in analogy with known procedures [18]. It was analyzed by GPC (Fig. 10, left part).

A marked enhancement of the molar masses was found when comparing the sample hydrolyzed before and that resulting from the exchange reaction. The major part of the latter distribution is sharp but the presence in the low molar masses of uncoupled polyethylene resulted in a 1.5 polydispersity index. An experiment similar to run 26 was performed with a lower ethylene amount. As expected, the product had short

Table 5
Applications of lanthanidocene/dialkyl-magnesium catalytic systems

| Entry | Name | Ethylene polymerization[a] | Second step reaction | Analyses |
|---|---|---|---|---|
| 24 | Homologation of undec-1-ene | Mg: 1 mmol, toluene: 0.1 L, $C_{11}H_{22}$: 10 mmol, temp.: 100 °C, 4 min | Hydrolysis | GC: odd and even $C_n$ distributions, 40/60 weight ratio |
| 25 | Polyethylenyl carboxylic acids | Mg: 10 mmol, toluene: 0.5 L, 5 min | $CO_2$ bubbling for 2 h, yield: 4.2 g | Mass spectrometry: distribution centered on $C_{13}$ acids. Satisfactory NMR and IR analyses |
| 26 | Star-shaped polymer | 25 min | $SnCl_4$: 2.5 mmol, 80 °C, 1 h, yield: 11.4 g | GPC: branches $M_n$=940 g/mol (PDI = 1.2), star polymer $M_n$ = 2560 g/mol (1.5), satisfactory NMR analyses |
| 27 | PE–PMMA copolymer | 30 min | MMA: 50 mmol, −78 °C, 2 h, yield: 16.7 g | GPC: PE block $M_n$=1040 g/mol (1.2), copolymer $M_n$=1450 g/mol (1.4), satisfactory IR analyses |
| 28 | PE–PεCL copolymer | 30 min | εCL: 500 mmol, 1 h, yield: 60 g | GPC: PE block $M_n$ = 1100 g/mol (1.2), copolymer $M_n$ = 4280 g/mol (12.7), satisfactory DSC and IR analyses |

[a] $(C_5Me_5)_2SmCl_2Li(OEt_2)_2$ **1b**: 0.1 mmol; butyl-ethyl-magnesium **2**: 5 mmol otherwise specified; solvent: Isopar 0.5 L otherwise specified; ethylene: 114 kPa; temperature: 80 °C otherwise specified.

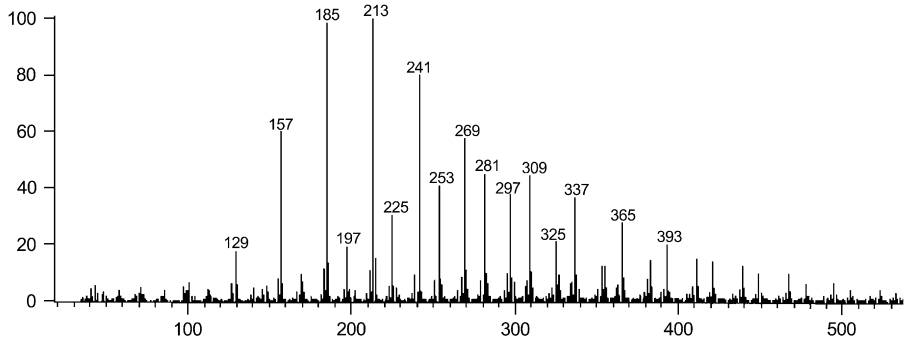


Fig. 9. Mass spectrum of the polyethylenyl carboxylic acids obtained for run 25 in Table 5.

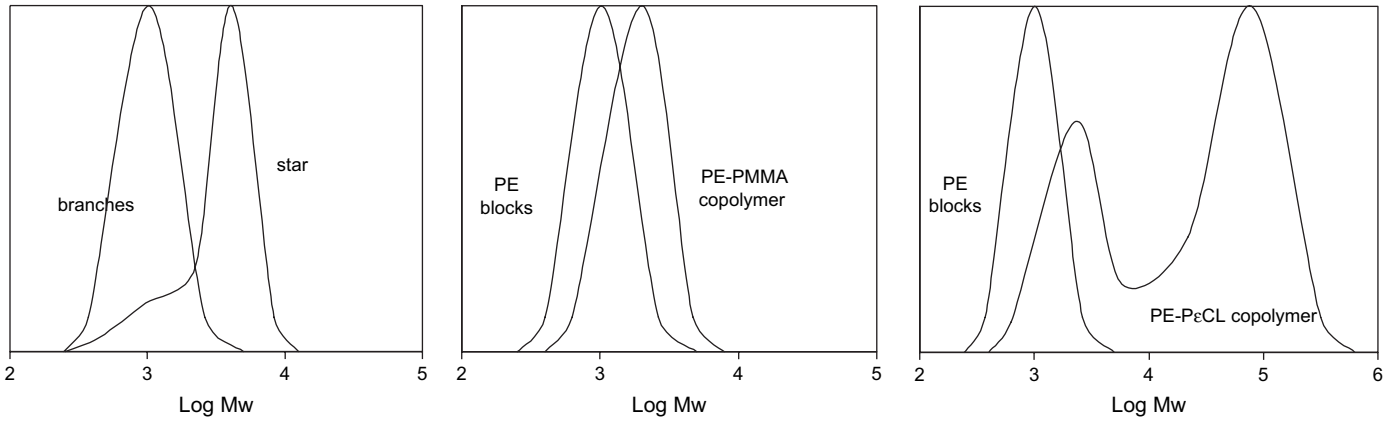


Fig. 10. GPC plots of the star-shaped polyethylene, the PE–PMMA and the PE–PεCL copolymers and the corresponding PE blocks obtained for runs 26–28 in Table 5.

branches and this allowed a better characterization of the chain ends and the core of the star-shaped product via $^{13}C$ NMR analysis (see Section 2). The data are consistent with a four-arm structure $(R-CH_2-)_4Sn$, together with a three-arm structure $(R-CH_2-)_3Sn$ in a 3/1 ratio.

Several studies describe successful copolymerizations by reaction of pure polyethylenyl-lanthanide compounds with polar monomers including methyl methacrylate and lactones [38]. In our case, block copolymerisations were run starting from polyethylenyl lanthanide and magnesium mixtures with methyl methacrylate and with ε-caprolactone. For methyl methacrylate, the experimental conditions of the second polymerization step have been chosen by analogy with published procedures of living anionic polymerization initiated with magnesium alkyls [39]. As can be seen in run 27 (Table 5), the molecular weight enhancement between the first block and the final product is consistent with the bonding of the two polymers (Fig. 10, middle part). A polar block with an average molecular weight of around 500 g/mol was successfully grafted on a polyethylene block with an average molecular weight of above 1000 g/mol. The polydispersity index remains satisfactory proving the living nature of the process. IR analyses confirmed the presence of both types of polymer in the residue of extraction with boiling acetone during 4 days in a Kumagawa apparatus. This means that the polar blocks, whose corresponding homopolymer is soluble in acetone, were grafted to sufficiently long blocks of non-polar polyethylene to become insoluble.

For ε-caprolactone, the second polymerization step was conducted at the same temperature as the ethylene polymerization step (see run 28 in Table 5). Large amounts of product were easily obtained. In this case, however, the GPC analysis of the crude product showed a bimodal distribution which results in a high overall polydispersity index (Fig. 10, right part). Such a situation should result from a two site catalytic process. Actually, lanthanides are among the most active catalysts for ring opening polymerization of lactones and lactide [40]. Hence, we suggest that the polyethylenyl lanthanide, although in minor amounts (1% of the polyethylenyl amount, Mg/Nd = 50), gives rise to a copolymer with a very long polyester block centered at 80,000 g/mol and accounting for 70% of the crude product weight (based on the area of the GPC curve). In contrast, polyethylenyl magnesium is much less reactive and gives rise to a copolymer with short polyester blocks since the PE block had $\overline{M}_n = 1100$ g/mol and the corresponding copolymer is centered at 2300 g/mol. According to these numbers, the PE block accounts for 48% of the low molar mass copolymer, while it accounts for only 1.4% in the high molar mass copolymer. Extraction of the crude product with boiling acetone during 8 days in a Kumagawa apparatus gave a residue accounting for 12% of the overall polymer, 40% of the low molar mass copolymer and was monodisperse

with $\overline{M}_w/\overline{M}_n = 1.3$. Analyses of the residue by DSC and IR spectroscopy revealed the presence of both types of polymer (PE and PCL). Hence, this residue also contains polycaprolactone blocks bearing sufficiently long blocks of non-polar polyethylene to be insoluble. It evidences that chemical bonding between PE and PCL is effective for the shortest chains.

### 3.10. Concluding remarks

We think that the most original results obtained with our system, i.e. stabilization of the active species and rapid exchange, are to be attributed to the presence of the dialkyl-magnesium compounds and alkyl-lanthanidocene compounds in associated structures. We suggest that β-hydrogen interactions (the key step for the elimination route [32]) may be disfavored with the lanthanide centers because of competition with the magnesium centers. Agostic interactions, particularly for hydrogen in β or γ positions are commonly observed in dialkyl-magnesium aggregates [41]. It is clear that the fast transfer process implies a fluxional behavior between the Ln/Mg and Mg/Mg alkyl bridges. What is still unknown is if these processes, especially the most important one involving Ln/Mg alkyl exchanges, are occurring via a dissociative or associative pathway. One possibility would be that this exchange would occur via a doubly bridged four-centered bimetallic complex, by the transient formation of $\eta^1/\eta^2$ coordinating $MgR_3^{\ominus}$ moieties (see the proposed alkyl exchange process in Scheme 1). An associative pathway via a multiple-bridged structure has been recently proposed in the case of rare-earth tetraalkyl-aluminate complexes [42]. The occurrence of a dissociative ionic pathway involving transient magnesiate anions is here less probable, as even if ionic compounds like $Cp^*_2Y^{\oplus}$, $^{\ominus}AlMe_4$ were identified at high temperature [10a], attempts at generating $Cp^*_2$Ln-R species using **1** and $AlEt_3$ as alkylating agent have led to inactive species. In this case, as well as in other **1**/alkylating reagents such as $Al(iBu)_3$, $LiAlH_4$, $ZnEt_2$ and MAO, no polymerization occurred [23a]. Butyl-lithium and phenyl-lithium gave polymerization, but without transfer when using an excess of these reactants. Therefore, we are confident that the major feature allowing the above reaction to occur in a propagation/transfer living process is *a close match* between $Cp^*_2$Ln-C and RMg-C bond strengths. This has to be taken into account in further research aimed at the discovery of any catalyzed chain growth reaction (CCG) [16b] via a fine tune of the metal(s) environment(s). Whether the alkyl exchange is occurring via magnesium–lanthanidocene, polynuclear aggregated species or simple dinuclear alkyl bridged complexes Ln–Mg is still an open question, for which the answer would only be clarified upon experiments leading to well-defined Ln/Mg species. Attempts at such reactions are currently under way in our laboratory.

## 4. Conclusion

The catalytic properties of the lanthanidocene/dialkyl-magnesium mixtures for ethylene polymerization were extensively studied by varying the most important parameters such as magnesium concentration and temperature. Observation of the ethylene consumption curves and careful analysis of the isolated polyethylene showed that under specific experimental conditions, this system could be considered as living. The specific properties of this peculiar catalytic system obtained by the lanthanidocene and dialkyl-magnesium mixture result from the specific characteristics of each component. The lanthanidocene complex is responsible for an excellent polymerization activity, while the dialkyl-magnesium compound stabilizes the active species and acts as a very efficient transfer agent. All of the alkyls provided by the magnesium compounds in excess could each initiate polymerization. Due to fast and reversible exchanges at 80 °C, all of them can grow steadily in an overall living process. This work affords an example of controlled polymerization based on equilibrium between active and dormant species with a coordination/insertion mechanism involving lanthanides and magnesium, and compares well with the recent work of Gibson based on iron/zinc catalyzed chain growth polymerizations, where monomeric diethyl-zinc acts as the transfer reagent. In our case, long chain dialkyl-magnesiums are produced similarly from butyl-ethyl-magnesium, although they are well known to be rather in aggregated structures than monomeric ones. As far as the application of these higher dialkyl-magnesiums is concerned, they behave as classical Grignard reagent. In this work, such functionalization by carbon dioxide has been performed and the block copolymerization with polar monomers by an anionic mechanism was successfully tested. This in situ alkylating method that affords lanthanide active species for polymerization also proved to be useful with other monomers [43], as well as using other lanthanidocene precursors [44] and alkylating agents [45]. It should also be emphasized that recently, this process has been successfully applied to produce alkoxyamine-terminated PE's and sulfur-functionalized PE's, useful as macroinitators for controlled radical polymerization and for RAFT polymerization, respectively [46]. Other applications could be the use of these Grignard compounds as reactants for grafting to dyes or to biologically active molecules to give them lipophilic properties via ponytail structures, and using the chain length control of the polymer for a fine tuning of the hydrophilic–lipophilic balance for the required application.

## Acknowledgements

We thank ECP EniChem Polymères France for their experimental assistance and financial support. Dr. Francine Agbossou-Niedercorn, Dr. Régis Gauvin and Pr. Marc Visseaux are gratefully acknowledged for helpful discussions.

## References

[1] For general reviews of organolanthanide polymerization catalysts:
(a) Gromada J, Carpentier JF, Mortreux A. Coord Chem Rev 2004; 248:397;
(b) Hou Z, Wakatsuki Y. Coord Chem Rev 2002;231:1.
[2] (a) Porri L, Ricci G, Giarrusso A, Shubin N, Lu Z. ACS Symp Ser 2000;749:15;

(b) Kaita S, Hou Z, Nishiura M, Doi Y, Kurazumi J, Horiuchi AC, et al. Macromol Rapid Commun 2003;24:179.
[3] (a) Okuda J, Arndt S, Beckerle K, Hultzsch KC, Voth P, Spaniol TP. In: Blom R, editor. Organometallics catalysts and olefin polymerization. Berlin: Springer–Verlag; 2001. p. 156–65;
(b) Kirillov E, Lehmann CW, Razavi A, Carpentier JF. J Am Chem Soc 2004;126:12240.
[4] Yasuda HJ. Organomet Chem 2002;647:128.
[5] Kaminsky W. In: Seymour RB, Cheng T, editors. History of polyolefins. Dordrecht: Reidel; 1986.
[6] (a) Watson PL. J Am Chem Soc 1982;104:337;
(b) Watson PL, Roe DC. J Am Chem Soc 1982;104:6474;
(c) Burger BJ, Thompson M, Cotter D, Bercaw JE. J Am Chem Soc 1990;112:1566;
(d) Casey CP, Hallenbeck SL, Wright JM, Landis CR. J Am Chem Soc 1997;119:9680;
(e) Klimpel MG, Eppinger J, Sirch P, Scherer W, Anwander R. Organometallics 2002;21:4021.
[7] Jordan RF, Bradley PK, La Pointe RE, Taylor DF. New J Chem 1990;14:505.
[8] (a) Watson PL, Herskowitz T. ACS Symp Ser [Initiation Polym] 1983; 212:459;
(b) Watson PL, Parshall GW. Acc Chem Res 1985;18:51;
(c) For analogous rare earth metallocene, see: Ballard DGH, Courtis A, Holton J, McMeeking J, Pearce R. J Chem Soc Chem Commun 1978; 994.
[9] Jeske G, Lauke H, Mauermann H, Swepston PN, Schumann H, Marks TJ. J Am Chem Soc 1985;107:8091.
[10] Fluxionality of tetra-alkyl-aluminate anion was observed by NMR in the following complexes:
(a) $Cp^*_2YMe_2AlMe_2$: Den Haan KH, Wielstra Y, Eshuis JJW, Teuben JHJ. Organomet Chem 1987;323:181;
(b) $Cp^*_2SmEt_2AlEt_2$: Evans WJ, Chamberlain LR, Ziller JW. J Am Chem Soc 1987;109:7209;
(c) $Cp_2LnR_2AlR_2$ (Ln = Y, Sc; R = Me, Et): Holton J, Lappert MF, Ballart DGH, Pearce R, Atwood JL, Hunter WE. J Chem Soc Dalton Trans 1979;1:45;
(d) $Cp^*_2YbMe_2AlMe_2$: Berg DJ, Andersen RA. Organometallics 2003; 22:627;
(e) rac-$[Me_2Si(2\text{-}Me\text{-}C_9H_5)_2]YMe_2AlMe_2$: see note ‖ in Ref. [42a];
(f) $(2,4,6\text{-Triisopropylbenzoate})_2LnMe_2AlMe_2$ (Ln = Y, La): see Ref. [42b].
[11] Ziegler K, Gellert HG, Külhorn H, Martin H, Meyer K, Nagel K, et al. Angew Chem 1952;64:323.
[12] Samsel EG. Eur Pat 539876, 1993 to Ethyl Corporation [Chem Abstr 1993;119:95815].
[13] Samsel EG, Eisenberg DC. Eur Pat 574854, 1993 to Ethyl Corporation. US Pat 5,276,220, 1994 to Ethyl Corporation [Chem Abstr 1994;121: 86240].
[14] (a) Mani G, Gabbaï FP. Organometallics 2004;23:4608;
(b) Mani G, Gabbai FP. Angew Chem Int Ed Engl 2004;43:2263;
(c) Bazan GC, Rogers JS, Fang CC. Organometallics 2001;20:2059;
(d) Rogers JS, Bazan GC. Chem Commun 2000;1209;
(e) Boone HW, Mullins MJ, Nickias PN, Snelgrove V. WO 02/42313 A2, 2002 to Dow Chemical Company [Chem Abstr 2002;137:6585].
[15] Kretschmer WP, Meetsma A, Hessen B, Schmalz T, Qayyum S, Kempe R. Chem Eur J 2006;12:8969.
[16] (a) van Meurs M, Britovsek GJP, Gibson VC, Cohen SA. J Am Chem Soc 2005;127:9913;
(b) Britovsek GJP, Cohen SA, Gibson VC, van Meurs M. J Am Chem Soc 2004;126:10701;
(c) Britovsek GJP, Cohen SA, Gibson VC, Maddox PJ, van Meurs M. Angew Chem Int Ed Engl 2002;41:489;
(d) Britovsek GJP, Cohen SA, Gibson VC. WO 2003/014046 A1, 2003 to BP Chemicals [Chem Abstr 2003;138:170673].
[17] Keim W, Chen Z, Shen Z. Catal Lett 1991;10:233.
[18] (a) Bogdanovic B, Bons P, Konstantinovic S, Schwickardi M, Westeppe U. Chem Ber 1993;126:1371;
(b) Sen A, Kim JS. WO 2000/073359 A1, 2000 to Exxonmobil Research and Engineering Company [Chem Abstr 2000;134:29796].
[19] Coates GE, Wade K. The main group elements. In: Coates GE, Green MLH, Wade K, editors. Organometallic compounds. 3rd ed., vol. 1. London: Methuen; 1969. p. 98.
[20] Szwarc M. J Polym Sci Part A Polym Chem 1999;37:873.
[21] Penczek S, Duda A, Szymanski R, Biela T. Macromol Symp 2000;153:1.
[22] Menoret S, Fontanille M, Deffieux A, Desbois P, Demeter J. Macromolecules 2002;35:4584.
[23] (a) Olonde X, Mortreux A, Petit F, Bujadoux K. J Mol Catal 1993;82:75;
(b) Bujadoux K, Olonde X, Mortreux A, Petit F. WO 93/07180 A1, 1993 to ECP Enichem Polymeres France [Chem Abstr 1993;119:271958].
[24] Pettijohn TM, Hsieh HL. US Pat 5,109,085, 1992 to Phillips Petroleum Company [Chem Abstr 1992;117:27425].
[25] (a) Pelletier JF, Mortreux A, Olonde X, Bujadoux K. Angew Chem Int Ed Engl 1996;35:1854;
(b) Pelletier JF, Bujadoux K, Olonde X, Adisson E, Mortreux A, Chenal T. Eur Pat 96 40 07 31.4-2110 to ECP Enichem Polymeres France. US Pat 5779942, 1998 to Enichem S.p.A. [Chem Abstr 1998;125:301844].
(c) Pelletier JF. PhD thesis, Lille; 1996.
[26] Tiley TD, Andersen RA. Inorg Chem 1981;20:3267.
[27] We checked that other higher linear dialkyl-magnesium compounds, for example the di-*n*-hexyl ones, react as the butyl-ethyl ones.
[28] Wang JS, Matyjaszewski K. J Am Chem Soc 1995;117:5614.
[29] Dubois P, Robert J, Teyssie P. Synthesis of polymers. In: Schlueter AD, editor. Materials science and technology, vol. 20. Weinheim: Wiley–VCH Verlag GmbH; 1999. p. 195–229.
[30] (a) Long DP, Bianconi PA. J Am Chem Soc 1996;118:12453;
(b) Evans WJ, Forrestal KJ, Ziller JW. Angew Chem Int Ed Engl 1997;36:774.
[31] Penczek S, Biela T, Duda A. Macromol Rapid Commun 2000;21:941.
[32] Casey PC, Tunge JA, Lee TY, Fagan MA. J Am Chem Soc 2003;125: 2641.
[33] (a) Watson PL. J Chem Soc Chem Commun 1983;276;
(b) Evans WJ, Ulibarri TA, Ziller JW. Organometallics 1991;10:134;
(c) Booij M, Meetsma A, Teuben JH. Organometallics 1991;10:3246;
(d) Booij M, Deelman BJ, Duchateau R, Postma DS, Meetsma A, Teuben JH. Organometallics 1993;12:3531.
[34] Evans WJ, Ulibarri TA, Ziller JW. J Am Chem Soc 1990;112:2314.
[35] Highlights about why propene is not polymerized by $Cp^*_2YH$:
(a) Sändig N, Koch W. Organometallics 2002;21:1861;
(b) Casey CP, Tunge JA, Fagan MA. J Organomet Chem 2002;663:91.
[36] Hessen B, Van der Heijden H. J Chem Soc 1996;18:1670.
[37] Evans WJ, DeCoster DM, Greaves J. Organometallics 1996;15:3210.
[38] Yasuda H. J Polym Sci Part A Polym Chem 2001;39:1955.
[39] Joh Y, Kotake Y. Macromolecules 1970;3:337.
[40] Baran J, Duda A, Kowalski A, Szymanski R, Penczek S. Macromol Symp 1997;123:93.
[41] Starowieyski KB, Lewinski J, Wozniak R, Lipkowski J, Chrost A. Organometallics 2003;22:2458.
[42] (a) Anwander R, Klimpel MG, Dietrich HM, Shorokov DJ, Scherer W. J Chem Soc Chem Commun 2003;1008;
(b) Fischbach A, Perdih F, Herdtweck E, Anwander R. Organometallics 2006;25:1626.
[43] Bogaert S, Carpentier JF, Chenal T, Mortreux A, Ricart G. Macromol Chem Phys 2000;201:1813.
[44] Bogaert S, Chenal T, Mortreux A, Nowogrocki G, Lehmann CW, Carpentier JF. Organometallics 2001;20:199.
[45] (a) Boisson C, Monteil R, Ribour D, Spitz R, Barbotin F. Macromol Chem Phys 2003;204:1747;
(b) Boisson C, Barbotin F, Spitz R. In: Sano T, Uozumi T, Nakatani H, Terano M, editors. Progress and development of catalytic olefin polymerization. Tokyo: Technology and Education Publishers; 2000. p. 75.
[46] (a) Godoy Lopez R, Boisson C, D'Agosto F, Spitz R, Boisson F, Bertin D, et al. Macromolecules 2004;37:3540;
(b) Godoy Lopez R, Boisson C, D'Agosto F, Spitz R, Boisson F, Gigmes D, et al. Macromol Rapid Commun 2006;27:173.